DESIGN OF A PRESSURE SENSOR FOR MONITORING OF POST-ENDOVASCULAR ANEURYSM REPAIR

A. T. Sepúlveda, A. J. Pontes, J. C. Viana, L. A. Rocha
Institute for Polymers and Composites/I3N, University of Minho, Braga, Portugal

Isa C. T. Santos
Instituto de Engenharia Mecânica e Gestão Industrial / Faculdade de Engenharia, Universidade do Porto, Porto, Portugal

F. Fachin, R. Guzmán de Villoria, B. L. Wardle
Department of Aeronautics and Astronautics, Massachusetts Institute of Technology, Cambridge, MA, U.S.A.

Keywords: Implantable pressure sensor, Aneurysms, Carbon nanotubes, Pressure sensor design.

Abstract: This paper introduces the design and fabrication process of a flexible pressure sensor for monitoring post-endovascular aneurysm repairs (EVAR). Biocompatible flexible PDMS membranes with embedded aligned carbon nanotubes (CNTs) with a conductivity of 11 $S.m^{-1}$ and elastic modulus of 2 MPa are used to build a LC network for passive telemetry readout-out. The pressure sensor has a modelled sensitivity 14fF/mmHg for a pressure range between 6-47 mmHg, in agreement with the required application. The pressure sensor, with a 250 μm thickness and total area of 1 cm^2, will be contained within the stent-graft and used to measure the pressure inside the aneurysm sac to detect complications related to the EVAR procedure.

1 INTRODUCTION

An aneurysm can be defined as a permanent and irreversible localized dilatation of an artery, having at least a 50% increase in diameter compared with a normal one. Aneurysms can appear anywhere but they most commonly occur in the aorta, as well as in arteries located at the base of the brain and in the legs.

Two treatments are currently available for the treatment of aneurysms: conventional surgical repair (open surgery) (Myers, Devine, Barras and Self, 2001) and endovascular aneurysm repair (EVAR) (Parodi, Palmaz, and Barone, 1991). The first involves making a relatively large incision in the abdomen and inserting a prosthetic graft to replace the damaged section of the aorta. This procedure can also be performed laparoscopically, either by hand-assisted laparoscopic surgery or total laparoscopic surgery. EVAR is a minimally invasive procedure in which a stent-graft is guided from the femoral artery to the affected artery segment in order to prevent wall rupture, thereby shielding the aneurysm from the blood pressure. This treatment is usually associated with less physiological derangement, lower morbidity and mortality, and more rapid recovery than open surgery (Chuter, Parodi, and Lawrence-Brown, 2004) but regular monitoring/surveillance to detect and prevent complications such as graft migration, stent fracture, endoleaks, enlargement of the aneurysm sac, and abdominal aortic aneurysm AAA rupture are required (Katzen and MacLean, 2006) after the procedure.

Comparing both approaches, EVAR is preferable as it is less stressful, it significantly reduces systemic complications (Rutherford and Krupski, 2004), and it has both lower costs associated with inpatient stay and less (or no) need for intensive care facilities during recovery (Myers et. al. 2001, Hayter, Bradshaw, Allen, Guduguntla and Hardman, 2005). The durability of open surgery, established with long-term follow-up studies, is excellent (Rutherford and Krupski, 2004), so good that there

T. Sepúlveda A., J. Pontes A., C. Viana J., A. Rocha L., C. T. Santos I., Fachin F., Guzmán de Villoria R. and L. Wardle B..
DESIGN OF A PRESSURE SENSOR FOR MONITORING OF POST-ENDOVASCULAR ANEURYSM REPAIR.
DOI: 10.5220/0003127400140022
In *Proceedings of the International Conference on Biomedical Electronics and Devices* (BIODEVICES-2011), pages 14-22
ISBN: 978-989-8425-37-9

is little or no requirement for long-term surveillance, in contrast with EVAR whose current results suggest that there is a need for increased surveillance and re-intervention (Hayter et al., 2005, Michaels, Drury, and Thomas, 2005, Greenhalgh, 2005). Considering the longer life expectancies and the rising public expectations for quality of life, the costs associated with follow-up can jeopardize EVAR's effectiveness.

The current surveillance protocol involves imaging at 1, 6, and 12 months after the procedure, and thereafter, on an annual basis (Milner, Kasirajan and Chaikof, 2006). In order to reduce and even eliminate these exams, new surveillance technologies are being investigated, with the most promising technique identified thus far being remote pressure sensing (Milner et al., 2006). Remote pressure sensing enables the measurement of both the systolic and diastolic pressures within the residual aneurysm sac at any given point in time. Thus far, the Impressure Sensor (Remon Medical Technologies, Israel) and the CardioMems EndoSure Wireless AAA Pressure Sensor (CardioMems, Inc, USA) have been evaluated for abdominal aortic aneurysms (AAA) (Milner et al., 2006, Springer, Günther, and Schmitz-Rode, 2007).

This work introduces a new pressure sensor for endotension measurement. The focus is on the use of a flexible substrate enabling the conformability of the sensor to the stent-graft and thus the aorta. Compared to currently available devices, this aspect brings several advantagessince the sensor can be attached to the stent-graft and delivered in a single procedure (as oposed to the requirement of two catheters for the CardioMems device) and it enables the placement of more than one sensor (a sensor cluster) contributing to a more comprehensive study of post-EVAR aneurysm evolution (that is currently not possible).

The contributions in this paper are divided in 5 sections. After an introduction to the topic, the required sensor specifications are derived followed by the development of an electro-mechanical pressure sensor model. Next, a new fabrication process for the realization of the flexible sensor is introduced and finally some experimental results and conclusions are presented.

2 SENSOR SPECIFICATIONS

Research on implantable pressure sensors is very active and has been supported and justified by the need of continuous pressure monitoring for patients with congestive heart failure, as an early diagnostic mechanism for some risk patients and for post-EVAR surveillance (Receveur, Lindemans, and de Rooij, 2007, Potkay, 2008). Implantable pressure sensors are typically categorized into extra-arterial blood pressure and intra-arterial blood pressure (Potkay, 2008) devices. Extra-arterial pressure sensors are placed around the blood vessel and perform an indirect pressure measurement through the wall or through the expansion and contraction of the artery, requiring however an invasive surgical procedure for their implant while the intra-arterial devices are in contact with the blood stream, inside of the blood vessels.

Potkay (2008) defined a set of requirements for pressure sensors according to the problem to be addressed. In the case of EVAR, the requirements of the pressure sensor are shown in Table 1.

Table 1: Requirements for post-EVAR surveillance (Potkay, 2008).

Characteristic	Value
Measurement location	Between graft and aneurysm wall
Typical values (mmHg)	20 to 90
Measurement range (mmHg)	20 to 250
Measurement resolution (mmHg)	1
Measurement absolute accuracy (mmHg)	5
Signal bandwidth (Hz)	0 to 80
Arterial diameter (mm)	15 to 40

After stent-graft placement, the aneurysm sac gets depressurized and the pressure drops down to a few mmHg. A numerical study performed by Li and Kleinstreuer (2006) shows that after EVAR the pressure inside the aneurysm sac is around 12% of the current luminal pressure. Therefore, if one wants to sense the luminal pressure value (which ranges typically between 60 – 160 mmHg) through the aneurysm sac pressure, the sensor must be able to measure pressures between 6-16 mmHg with a resolution of 0.1 mmHg. In addition, the sensor needs a high dynamic range in order to detect stent-graft complications (in this case the sac gets pressurized and pressure increases to the luminal pressure values).

2.1 Telemetry System

The pressure monitoring system under development uses a passive telemetry system, based on an

implantable LC resonant network, for the external readout of the pressure sensor signal. The use of passive telemetry in implantable medical devices is well established (Mokwa, 2007) and enables the realization of active implants with no power constraints. A circuit representation of the sensor system and external reader, using the transformer model (parasitic capacitance is not included), is presented in Figure 1. The components in the sensor are modelled as passive elements: a variable capacitor C_s whose value changes with the applied pressure, connected to an inductor L_s, resulting in a parallel resonant circuit. The schematic representation in Figure 1 includes also the resistors R_p and R_s which model the parasitic elements associated with the inductors L_p and L_s and the capacitor C_s.

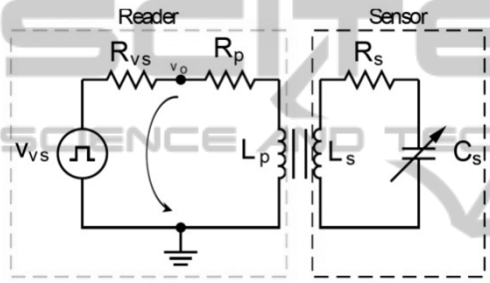

Figure 1: Telemetry circuit.

If the transformer is replaced by its T model, the following expression for the oscillating frequency is obtained:

$$f_{osc} = \frac{1}{2\pi\sqrt{\left(1-k^2\right)L_s C_s}}, \qquad (1)$$

where k represents the coupling coefficient of the transformer.

The system oscillation frequency was chosen to operate in the frequency band from 12.5 to 20.0 MHz, allocated specifically for medical applications. This frequency band presents additional advantages, unlike low operational frequencies, since the inductors and capacitors require small dimensions and therefore small sensors' area. Assuming a k = 0.06 (expected value for a distance of 5cm between the sensor system and the external reader) Equation 1 is used to assess the capacitance and inductor values required for the chosen frequency band. The results are presented in Figure 2.

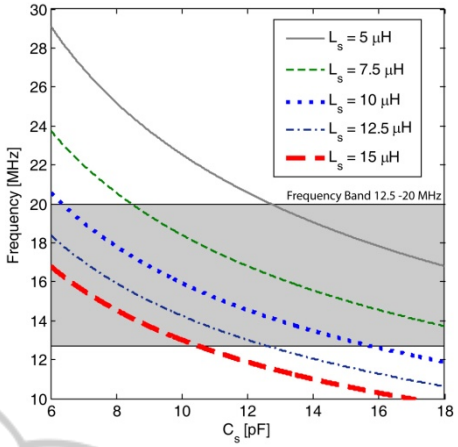

Figure 2: Telemetry system oscillating frequency vs. capacitance for several inductor values.

A detailed analysis as that shown in Figure 2 reveals that for inductors ranging from 5 to 15 µH, the capacitive changes should be between 5 and 18 pF to be within the chosen frequency band. The external reader is expected to have a resolution better than 1 kHz. If an inductor of 12.5 µH is used during the design of the sensor, the capacitive pressure sensor changes should be within the interval 5-12 pF for pressure variations between 6 to 120 mmHg.

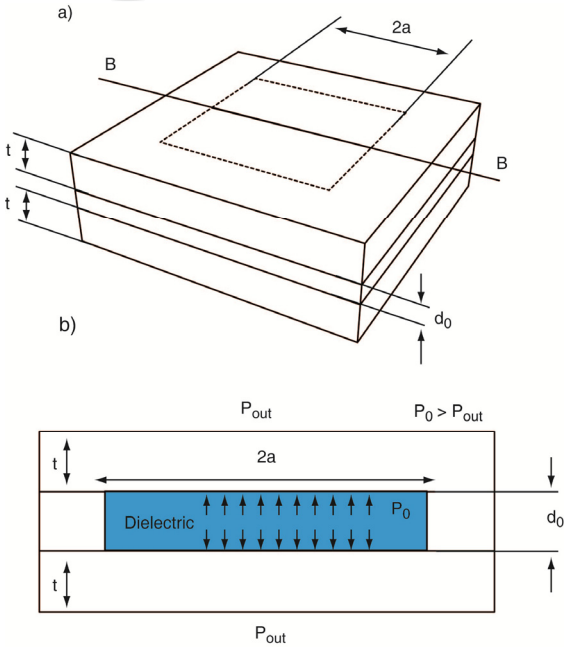

Figure 3: Schematic of the pressure square (sidelength = *2a*) sensor a) 3D view and b) section cut B-B.

3 PRESSURE SENSOR MODEL

The proposed pressure sensor is based on two square-plate (diaphragm) electrodes separated by a dielectric (air, at a pressure P_0). Changes on the outside pressure (P_{out}) deform the square plate and consequently generate a capacitive change. A schematic of the square platform (sidelenght of *2a*) pressure sensor is shown in Figure 3.

The sensor involves two coupled domains, mechanical and electrical, that define the sensor behaviour. An analysis of the behaviour of the two domains leading to the final model is performed next.

3.1 Mechanical Domain

The starting point to build the analytical model is the generic square diaphragm described in Figure 4 where a is the sidelength, t is the thickness and y_0 is the deflection. The diaphragm is clamped at the edges.

For a clamped diaphragm under a uniform load (like pressure), the angle of deflection, φ, can be defined as equal to zero at the center ($r = 0$) and at the edge ($r = a$) of the diaphragm. For these boundary conditions, the deflection of a square diaphragm under a pressure load can be modelled by (Chau and Wise, 1987):

$$P_0 - P_{out} = \frac{Et^4}{(1-\upsilon^2)a^4}\left[4.20\frac{y_0}{t} + 1.58\frac{y_0^3}{t^3}\right] \quad (2)$$

where υ is the Poisson's ratio, E is the Young's modulus, and $\Delta P = P_0 - P_{out}$ is the pressure load.

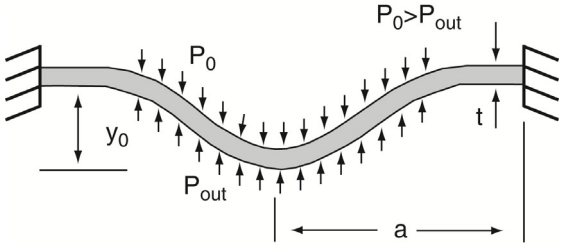

Figure 4: Generic model for a deflectable diaphragm.

Equation (2) allows the calculation of the deflection at the center of the diaphragm for a given pressure load, but, the deflection along the diaphragm is still required to model the capacitive changes due to gap variation. The complexity of the mechanical deflection model makes it difficult to obtain a closed form solution for the deflection of the diaphragm from the center to the edges. Assuming large deflections (expected due to the elasticity and low Young's Modulus of the flexible membranes) a circular deflection is considered and introduced here as:

$$y(r) = y_0 \sin\left(\arccos\left(\frac{r}{a}\right)\right) \quad (3)$$

Although the profile given by equation (3) might introduce some errors, it enables the calculation of a closed form expression for the changes in the capacitor.

3.2 Electrostatic Domain

A capacitor is an electronic component with two electrodes that are separated by a dielectric. For the simple case of a parallel plate capacitor, and in the absence of displacements, the model for the capacitor is:

$$C = \varepsilon_0 \varepsilon_r \frac{wl}{d_0}, \quad (4)$$

where ε_0 is the permittivity of free space (*8.8546x10-12 F/m*), ε_r is the relative permittivity, w and l are the width and length of the capacitor electrodes, and d_0 is the gap between the electrodes.

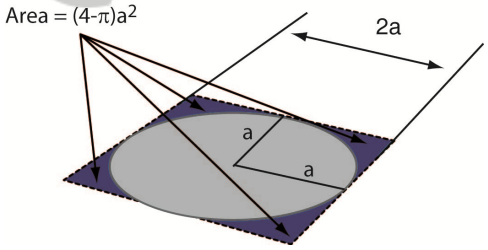

Figure 5: Area of a circular diaphragm vs. square diaphragm.

Since the capacitive sensor proposed here uses diaphragm electrodes with a complex bending profile, integration over the effective area of the electrodes is required to compute the total capacitance:

$$C = \int\int \frac{\varepsilon_0 \varepsilon_r}{d_0 + 2d(x,y)} dxdy, \quad (5)$$

where $d(x,y)$ is the distance between electrodes due to the diaphragm bending at position x, y. The integration of the bending profile of a square diaphragm is a complex exercise, and therefore, an interesting solution is to consider a circular diaphragm and use integration along the radius to

compute the capacitance (see Figure 5). With this simplification and replacing *d(x,y)* in equation (5) for *y(r)* yields for the capacitor model:

$$C_d = \int_0^{2\pi}\int_0^a \frac{\varepsilon_0\varepsilon_r}{d_0 + 2y_0 \sin\left(\arccos\left(\frac{r}{a}\right)\right)} r dr d\theta = \quad (6)$$

$$C_d = \varepsilon_0\varepsilon_r \frac{a^2\pi\left(d_0\left(\ln(d_0) - \ln(d_0 + 2y_0) + 2y_0\right)\right)}{2y_0^2}$$

The total capacitance, considering the areas not covered by the circular diaphragm, and assuming an average bending at the corners of 8% of the total bending is:

$$C_{total} = C_d + \varepsilon_0\varepsilon_r \frac{(4-\pi)a^2}{d_0 + 0.08y_0} \quad (7)$$

4 FABRICATION PROCESS

Given the characteristics of the application (the sensor will be attached to the stent-graft) the capacitive sensor must be foldable, extremely flexible and characterized by a very small profile. In addition, the technology should be simple and biocompatible. Silicon based microtechnologies are widely used in implantable medical devices (Receveur et al., 2007), but due to the application specifications, a new fabrication process is being developed.

The proposed fabrication process uses aligned carbon nanotubes (CNTs) to build the conductive elements, namely the inductor and the capacitor electrodes. The CNTs are embedded in a flexible substrate of polydimethylsiloxane (PDMS), a transparent, nontoxic and biocompatible silicone elastomer.

The fabrication process flow for the development of the flexible pressure sensor is schematically presented in Figure 6. Acrylic moulds are produced by CNC milling (Figure 6a) for posterior fabrication of the PDMS membranes. This technique has low costs and fast production times, but it is associated with poor dimensional control (dimensions less than 50μm are difficult to achieve).

The electrical components (capacitor electrodes and inductor) are based on aligned CNTs, as shown in Figure 6b. Chemical vapour deposition (CVD) is used to grow forests or "carpets" of vertically-aligned CNTs (Bello, Hart, Ahn, Hallock, Yamamoto, Garcia, Ellenbecker and Wardle, 2008).

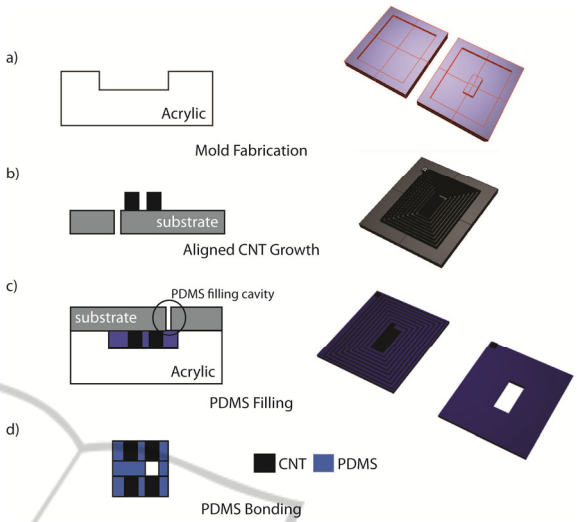

Figure 6: Fabrication process flow for the development of a flexible pressure sensor with aligned-CNT/PDMS nanocomposites.

A silicon substrate with patterned Fe/Al_2O_3 catalyst is placed on a horizontal quartz tube furnace at atmospheric pressure at 750 ºC (Hart, and Slocum, 2006) for the CNT growth. This method has the advantage of allowing growth of high purity, high yield and vertically aligned morphology. Next, the CNTs are embedded into the polymer matrix (PDMS). This step is schematically represented in Figure 6c. The substrate is placed against the moulds, and the PDMS is introduced in the cavities through a hole, followed by the curing of the elastomer.

The flexible pressure sensor is composed of three thin layers, with the top and bottom layers defining the inductor and the electrodes, and the middle one defining the dielectric (air). This configuration requires bonding of PDMS membranes. Eddings, Johnson and Gale (2008) tested five different bonding techniques and the highest reported bond strength was obtained for both partial curing and uncured PDMS adhesive techniques. The latter approach has proven successful in our work as well, and will be used for future experimentation.

5 RESULTS AND DISCUSSION

The key step of the fabrication process is the CNT-PDMS impregnation and respective mechanical and electrical properties (required for the sensor design). Acrylic moulds have been fabricated (Figure 7), and are being used to build the PDMS flexible membranes with embedded CNTs (Figure 8).

Aligned CNTs are oriented in the out-of-plane (or normal to the wafer plane) direction such that the polymer nanocomposite can be presumed transversely isotropic, *i.e.,* isotropic in the plane of the sensor. Furthermore, the modulus enhancement due to CNTs is likely minimal as the long axis of the CNTs are oriented perpendicular to the loading direction, such that the PDMS polymer dominates the response. Recent work has shown significant increase in modulus due to aligned CNTs in polymer (PDMS) (Ajayan et al., 2000) and epoxy (Cebeci et al., 2009) in the CNT axis direction, but little reinforcement effect in the transverse direction as used here. This result is expected from composite micromechanics analyses and experimental results.

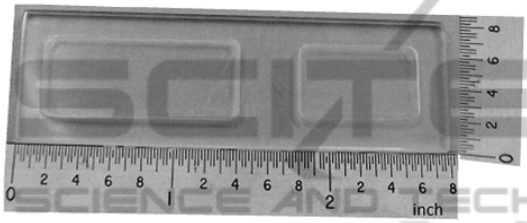

Figure 7: Fabricated acrylic moulds for the production of PDMS membranes.

a)

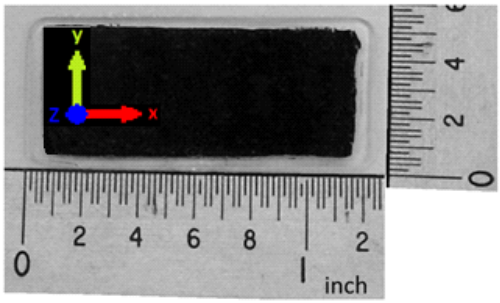

b)

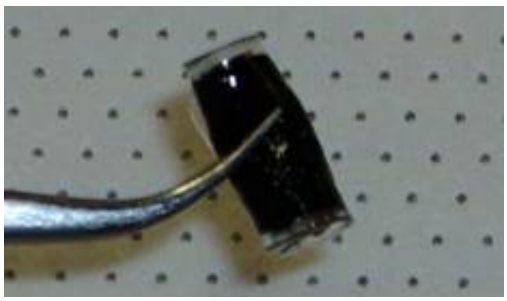

Figure 8: PDMS membrane with embedded aligned CNTs a) normal (the "z" axis corresponds to the direction of CNTs) and b) folded.

5.1 Electrical and Mechanical Characterization

Preliminary measurements of a series of PNC samples (PDMS membranes with embedded CNTs) indicate an electrical conductivity of *11.43* $S.m^{-1}$ with a standard deviation of *13.37* $S.m^{-1}$. The relatively high value of the standard deviation is related to the manual process being used for the membrane fabrication which gives origin to some imperfections.

Some other samples where subject to mechanical tests to obtain the elastic modulus and tensile strength. The PDMS/CNTs specimens were moulded into rectangular shapes with dimensions of 32 x 14 x 0.4 mm^3 (L x W x H), as shown in Figure 8a. The tensile tests were performed on a Zwick Z010 machine with a 500 N load-cell and extension rate of 1 mm/min for all specimens. Through the measured stress-strain curve, both the elastic modulus and tensile strength can be determined. Figure 9 shows an exemplary stress-strain curve of PDMS/CNTs membrane which has ~1% CNTs by volume oriented perpendicular to the loading direction. The tested membranes present an elastic modulus of about 2.42 MPa (at the initial stage) and rupture at around 0.87MPa. The pure PDMS has a Young modulus of approximately 0.5 MPa.

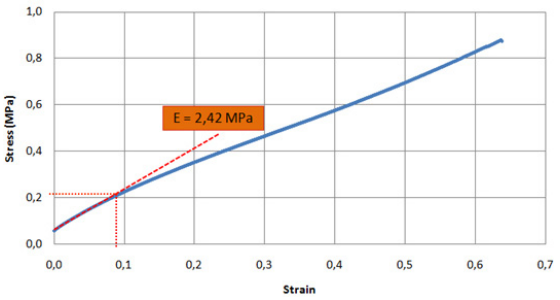

Figure 9: Stress-Strain curve of a flexible PDMS membrane with embedded CNTs.

5.2 Sensor Geometry

Equations (6) and (2) enable us to analytically calculate the capacitance changes for a given applied pressure on the sensor. An analytical model was implemented using the two equations and was used to design the sensor. The main concerns during the design phase were related to the device thickness (<=300 μm) and the capacitor total area (<=1.5 cm^2).

Table 2: Dimensions and material properties of the pressure sensor.

Parameter	Description	Value
a	radius	5 mm
d_0	distance between electrodes	50 μm
P_0	Pressure of the sensor cavity	8000 Pa
t	diaphragm thickness	100 μm
E	Elastic Modulus	2.42 MPa
υ	Poisson's ratio	0.48
ε_r	relative permittivity	1
ε_0	permittivity of free space	8.854×10^{-12} F/m

An important characteristic of the sensor behaviour is the sensitivity dependence on the dielectric cavity pressure (P_0). If the last bonding step is performed in a pressure controlled environment, P_0 can be controlled which allows the realization of sensors with different sensitivities and dynamic ranges. Table 2 presents the defined sensor dimensions taking into account that for this application, the pressure range to be measured is around 6-16 mmHg, while Figure 10 presents the expected capacitance changes using the analytical model.

In order to validate the model, a Finite Element Model (FEM) was developed in ANSYS using a coupled domain (mechanical and electrostatic) approach. The developed FEM model uses initially a structural physical domain that computes the bending due to applied pressure. Then, the command *dvmorph* is issued and the non-structural areas are re-meshed (taking into account the displacement of the diaphragm due to pressure applied). Finally, an electrostatic physical domain is used to calculate the capacitance. The comparative results are presented in Figure 10. The deviations between models are due to the assumptions made during the derivation of the analytical model.

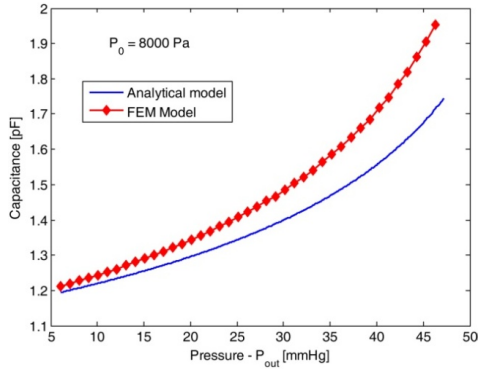

Figure 10: Capacitance changes due to external pressure changes.

Figure 11a shows the bending of the diaphragm for an external pressure of 6mmHg and Figure 11b the stress on the membranes.

5.3 Discussion

The results obtained raise three main concerns regarding the suitability of the realization of a pressure sensor with passive telemetry using the proposed technology. The first one is related to the rather low conductivity of the PDMS membranes with embedded CNTs. The low conductivity will generate a rather high resistance of the inductor and therefore the energy transferred inductively will be dissipated in the resistor. Solutions to overcome this problem are already being studied, and the use of inkjet-printed conductive inks seems to be a good candidate. Alignment of the continuous CNTs in the conduction direction is another option, as much higher conductivities have been reported for PNCs.

A second concern is the low capacitive value (1-2pF) of the proposed sensor geometry. While the capacitive changes are within the desirable values, the total capacitor value is lower than the required one (see section 2). This problem can be easily overcome by placing a fixed capacitor in parallel (using the middle PDMS layer as dielectric) in such a way that the total capacitance value is within the required values (5-12pF). PNC morphology changes may also be used to engineer this quantity as with electrical resistivity above.

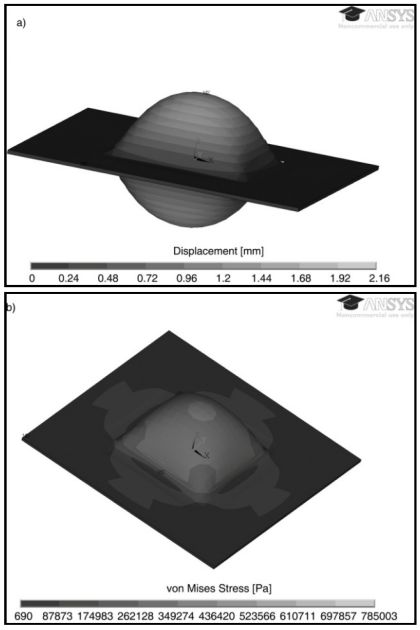

Figure 11: Results from the FEM model a) bending and b) von Mises stress contours.

The third concern relates to the tensile strength of the membranes. The measured rupture stress of the samples (~0.87 MPa) is within the range of stresses given by the FEM model. While the stresses on the diaphragm are well below this value, the stresses retrieved from the FEM model on the edges of the diaphragm approach the membranes tensile strength meaning that the devices can break during operation. A solution to reduce the stress in the edges could be to work on the mould in order to avoid sharp edges (where stresses tend to accumulate). Alternatively, one could try to increase the tensile strength of the membranes by changing the volume fraction and/or configuration of the embedded aligned CNTs.

6 CONCLUSIONS

This paper introduces a new approach for the pressure measurement within an aneurysm sac for post-EVAR surveillance based on a highly flexible pressure sensor. The pressure sensor is flexible and thin so it can be placed on top of a stent-graft and delivered during the EVAR procedure without the requirement of an extra surgery step.

The characterization results of the new introduced fabrication process are promising and enable the realization of a pressure sensor that has the required specifications (sensitivity and dynamic range) for the application. Nevertheless, some problems are foreseen that can jeopardize the final implementation. This technology can find applications in other fields such as e-textiles and portable medical devices, opening the scope of the current research.

The first sensor prototypes are under development, and fully sensor characterization is expected soon.

ACKNOWLEDGEMENTS

The first author wishes to thank FCT - Fundação para a Ciência e Tecnologia, Portugal, for the financial support provided by the grant SFRH/BD/ 42922/2008. This work is supported by FCT under the project MIT-Pt/EDAM-EMD/0007/2008. CNT-based polymer composite materials were developed with funding from Airbus S. A. S., Boeing, Embraer, Lockheed Martin, Saab AB, Spirit AeroSystems, Textron Inc., Composite Systems Technology, and TohoTenax Inc. through MIT's Nano-Engineered Composite aerospace STructures (NECST) Consortium.

REFERENCES

Ajayan, P. M., Schadler, L. S., Giannaris, C. and Rubio, A. (2000), Single-Walled Carbon Nanotube–Polymer Composites: Strength and Weakness. *Advanced Materials*, 12, 750-753.

Bello, D., Hart, A. J., Ahn, K., Hallock, M., Yamamoto, N., Garcia, E. J., Ellenbecker, M. J., Wardle, B. L. (2008). Particle exposure levels during CVD growth and subsequent handling of vertically-aligned carbon nanotube films. *Carbon*, 46, 974-977.

Cebeci, H., Guzmán de Villoria, R., Hart, A. J., and B. L. Wardle (2009). Multifunctional Properties of High Volume Fraction Aligned Carbon Nanotube Polymer Composites with Controlled Morphology. *Composites Science and Technology*, 69, 2649-2656.

Chau, H.-L. and Wise, K. D. (1987). Scaling limits in batch-fabricated silicon pressure sensors. *IEEE Trans. Electron Devices ED*, 24, 850–858.

Chuter, T., Parodi, J. C. and Lawrence-Brown, M. (2004). Management of abdominal aortic aneurysm: a decade of progress. *Journal of Endovascular Therapy*, 11(Suppl II), S82-S95.

Eddings, M. A., Johnson, M. A., Gale, B. K. (2008). Determining the optimal PDMS-PDMS bonding technique for microfluidic devices. *J. Micromech. Microeng.* 18, 067001.

Greenhalgh, R. M. (2005). Endovascular aneurysm repair versus open repair in patients with abdominal aortic aneurysm (EVAR trial 1): randomised controlled trial. *Lancet*, 365(9478), 2179-2186.

Hart, J., Slocum, A. H. (2006). Rapid growth and flow-mediated nucleation of millimeter-scale aligned carbon nanotube structures from a thin-film cata-lyst. *Journal of Physical Chemistry B*, 110, 8250-8257.

Hayter C. L., Bradshaw S. R., Allen R. J., Guduguntla M. and Hardman D. T. (2005). Follow-up costs increase the cost disparity between endovascular and open abdominal aortic aneurysm repair. *Journal of Vascular Surgery*, 42(5), 912-918.

Katzen, B. T. and MacLean, A. A. (2006). Complications of endovascular repair of abdominal aortic aneurysms: A review. *CardioVascular and Interventional Radiology*, 29(6), 935-946.

Li, Z. and Kleinstreuer, C. (2006). Analysis of biomechanical factors affecting stent-graft migration in an abdominal aortic aneurysm model. *J. of Biomechanics*, 39 (12), 2264-73.

Michaels, J. A., Drury, D. and Thomas, S. M. (2005). Cost-effectiveness of endovascular abdominal aortic aneurysm repair. *British Journal of Surgery*, 92, 960-967.

Milner, R., Kasirajan, K. and Chaikof, E. L. (2006). Future of endograft surveillance. *Seminars in Vascular Surgery*, 19(2), 75-82.

Mokwa, W. (2007). Medical implants based on Microsystems. *Meas. Sci. Technol.,* 18, R47-R57.

Myers, K., Devine, T., Barras, C., Self, G. (2001). Endoluminal Versus Open repair for abdominal aortic aneurysms. *2nd Virtual Congress of Cardiology*.

Parodi, J. C., Palmaz, J. C. and Barone, H. D. (1991). Transfemoral intraluminal graft implantation for abdominal aortic aneurysms. *Annals of Vascular Surgery*, 5(6), 491-499.

Potkay, J. A. (2008). Long term, implantable blood pressure monitoring systems. *Biomed Microdevices*, 10, 379–392.

Receveur, R. A. M., Lindemans, F. W. and de Rooij, N .F. (2007). Microsystems technologies for implantable applications. *J. Micromech. Microeng.*, 17, R50-R80.

Rutherford, R. B. and Krupski, W. C. (2004). Current status of open versus endovascular stent-graft repair of abdominal aortic aneurysm. *Journal of Vascular Surgery*, 39(5), 1129-1139.

Springer, F., Günther, R. W. and Schmitz-Rode, T. (2007). Aneurysm sac pressure measurement with minimally invasive implantable pressure sensors: An alternative to current surveillance regimes after EVAR?. *CardioVascular and Interventional Radiology*, 31(3), 460-467.